Scientific Data

https://doi.org/10.1038/s41597-026-07846-4

Article in Press

Long-term crop mapping in the three provinces of Northeast China based on multi-source sample fusion

Received: 23 January 2026

Accepted: 6 July 2026

Published online: 21 July 2026

Cite this article as: Bai, Z., Gao, M., Feng, F. *et al.* Long-term crop mapping in the three provinces of Northeast China based on multi-source sample fusion. *Sci Data* (2026). https://doi.org/10.1038/s41597-026-07846-4

Zhaoyang Bai, Maofang Gao, Fukang Feng, Shilei Li, Qiang Li, Guofei Shang, Jianxi Huang, Zhao-Liang Li, Xia Zhang, Gianfausto Bottini & Francesco N. Tubiello

We are providing an unedited version of this manuscript to give early access to its findings. Before final publication, the manuscript will undergo further editing. Please note there may be errors present which affect the content, and all legal disclaimers apply.

If this paper is publishing under a Transparent Peer Review model then Peer Review reports will publish with the final article.

ARTICLE IN PRESS

© The Author(s) 2026. **Open Access** This article is licensed under a Creative Commons Attribution-NonCommercial-NoDerivatives 4.0 International License, which permits any non-commercial use, sharing, distribution and reproduction in any medium or format, as long as you give appropriate credit to the original author(s) and the source, provide a link to the Creative Commons licence, and indicate if you modified the licensed material. You do not have permission under this licence to share adapted material derived from this article or parts of it. The images or other third party material in this article are included in the article's Creative Commons licence, unless indicated otherwise in a credit line to the material. If material is not included in the article's Creative Commons licence and your intended use is not permitted by statutory regulation or exceeds the permitted use, you will need to obtain permission directly from the copyright holder. To view a copy of this licence, visit http://creativecommons.org/licenses/by-nc-nd/4.0/.

ARTICLE IN PRESS

Long-term crop mapping in the three provinces of Northeast China based on multi-source sample fusion

Zhaoyang Bai[1,2], Maofang Gao[1*], Fukang Feng[3], Shilei Li[1], Qiang Li[1], Guofei Shang[2], Jianxi Huang[4], Zhao-Liang Li[2,1*], Xia Zhang[2], Gianfausto Bottini[5] and Francesco N. Tubiello[5]

[1] State Key Laboratory of Efficient Utilization of Arable Land in Northern China, Institute of Agricultural Resources and Regional Planning, Chinese Academy of Agricultural Sciences, Beijing 100081, China;

[2] Hebei International Joint Research Center for Remote Sensing of Agricultural Drought Monitoring / School of Land Science and Space Planning，Hebei GEO University, Shijiazhuang, 050031, China;

[3] School of Marine Sciences, Sun Yat-sen University, Guangzhou 510275, China;

[4] Faculty of Geosciences and Engineering, Southwest Jiaotong University, Chengdu 611756, China

[5] Statistics Division, Food and Agriculture Organization of the United Nations, Rome, Italy

[*] Corresponding author: gaomaofang@caas.cn: Maofang Gao; lizhaoliang@caas.cn: Zhao-Liang Li

ARTICLE IN PRESS

Abstract

The Northeast region serves as a vital grain production base in China, with an increasingly prominent role in national food security. This study integrated existing crop classification products and land cover data to extract samples of rice, maize, soybean, and other land cover types within Northeast China covering the period 1985-2024. An inter-annual sample migration method based on Spectral Angle Mapper (SAM) was adopted to construct a comprehensive sample database, to be used as input for crop type classification, covering the entire study period. By leveraging Landsat imagery and applying the Random Forest algorithm, we generated 30-meter-resolution crop maps for rice, maize, and soybean from 1985 to 2024. The resulting maps achieved high accuracy, with crop area estimates highly consistent with municipal-level statistical data. Among the three provinces, the maximum overall accuracy and Kappa coefficient could reach 0.99. Liaoning Province achieved the best average classification accuracy, with mean overall accuracy and Kappa values of 0.87 and 0.81, respectively. These findings provide a robust data foundation for ensuring food security and informing agricultural management strategies.

Keywords: multi-source sample; long time series; crop mapping; Northeast China

Background & Summary

ARTICLE IN PRESS

Food security is a critical global concern, and the optimization of cropping structure is fundamental to ensuring regional food security. As one of the world's largest agricultural producers, China has experienced continuous changes in its cropping systems driven by policy interventions, market dynamics, and climate variability[1]. Northeast China, one of the country's most important grain-producing regions, plays a pivotal role, where changes in the distribution of major crops such as rice, maize, and soybean have significant implications for national food security. In this context, accurate identification of crop types, cropping patterns, and their interannual dynamics is essential for understanding agricultural system evolution and assessing food security[2].

In recent years, substantial progress has been made in crop type mapping at the national scale in China, driven by advances in remote sensing data and computational methods. Existing studies have developed nationwide datasets of crop distribution[3,4] and cropping systems[5] using multi-source data such as Landsat, MODIS, and Sentinel, providing valuable insights into large-scale agricultural patterns. However, these products remain constrained by spatial resolution and temporal consistency, limiting their ability to capture complex cropping structures and rotation systems at regional scales.

At the regional scale, extensive efforts have been devoted to crop mapping in Northeast China. For example, long-term maize maps at 30 m resolution are available for 2000-2021[6-8], while rice datasets span from 1990 to 2022 with spatial resolutions up to 20 m[9,10]. In contrast, long-term soybean mapping remains relatively limited, with available datasets mainly covering 2017-2021 at approximately 10 m resolution[11]. In addition, previous studies have examined regional crop distribution and its dynamics. These efforts have substantially improved the accuracy and temporal continuity of single-crop mapping and provided important data support for regional agricultural studies.

Despite these advances, several key limitations remain. On the one hand, national-scale datasets lack sufficient spatial detail and regional adaptability to support fine-scale analyses. On the other hand, regional studies, although high in spatial resolution, are predominantly focused on single crops. Differences in classification schemes, mapping criteria, and inherent uncertainties across datasets hinder their direct integration[6,12,13]. Moreover, the absence of multi-crop datasets developed under a unified classification framework and consistent spatiotemporal resolution limits systematic analysis of cropping structure and rotation patterns. As a result, comprehensive assessments of long-term agricultural system dynamics—particularly in response to policy interventions, water resource constraints, and market changes—remain insufficient. There is therefore a clear need for a harmonized, long-term, multi-crop dataset to support integrated regional analyses.

This study aims to develop a high-resolution dataset to characterize the co-distribution of maize, soybean, and rice in Northeast China over the past four decades (1985-2024). To achieve this, we first integrated multiple existing crop products to derive reliable training samples, and then combined them

ARTICLE IN PRESS

ARTICLE IN PRESS

with long-term Landsat observations from Landsat-4/5/7/8/9. Vegetation indices were used as input features, and a random forest (RF) algorithm was applied for monthly classification and probability estimation. Compared with existing multi-crop mapping efforts, the main contribution of this dataset lies in its extended temporal coverage and cross-period consistency, providing a robust data foundation for analyzing long-term changes in cropping systems.

Methods

The overall technical workflow of this study is illustrated in Fig. 1. First, time-series Landsat images were preprocessed through radiometric calibration, cloud masking, and monthly composite generation. Subsequently, multiple band information and spectral indices were extracted and calculated for crop mapping. Second, existing crop classification products were integrated, and random sampling was performed. Non-crop samples were supplemented from land cover products, and a sample migration method based on the SAM method was applied to construct a multi-source sample database. Finally, multiple independent RF models were trained using these samples, with each model generating a crop distribution probability map. These probability maps were temporally fused by averaging monthly category probabilities through pixel-wise accumulation. The final crop classification for each pixel was determined based on the maximum average probability, resulting in the ultimate crop distribution map.

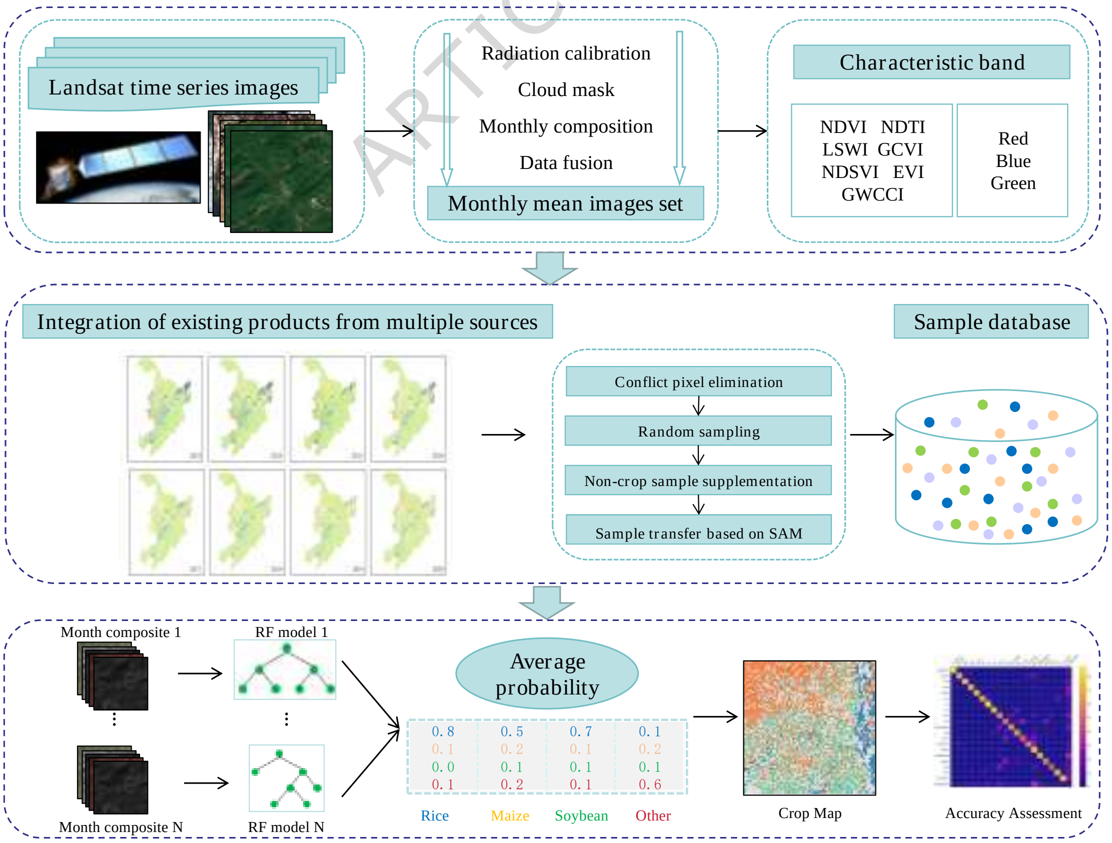

Figure 1. Workflow of this study.

Study area

The study area is located in Northeast China, extending from approximately 38°N, 118°E to 54°N, 136°E. It primarily includes Heilongjiang Province (HLJ), Jilin Province (JL), and Liaoning Province (LN) (Fig. 2), covering a total area of about 787,000 km². This region represents approximately 8% of China's total land area[14,15].The cropland area in this region covers 26,400 square kilometers, accounting for approximately 16 percent of China's total cropland. The Northeast Region is renowned as one of the three world's famous "Black Soil Regions". The main crops grown in this area currently are maize, soybean, and rice[13]. The combined planting area of these three crops exceeds 90% of the total cropland area[6]. The region is known in China as the "Golden Maize Belt" and the "Hometown of Soybean". It experiences a temperate monsoon climate with four distinct seasons. Winters are typically long and cold, while summers are short and warm. Annual precipitation ranges from 500 mm to 800 mm, with the majority occurring during the summer months. Due to these climatic characteristics, a single-cropping system is generally practiced throughout the region[16].

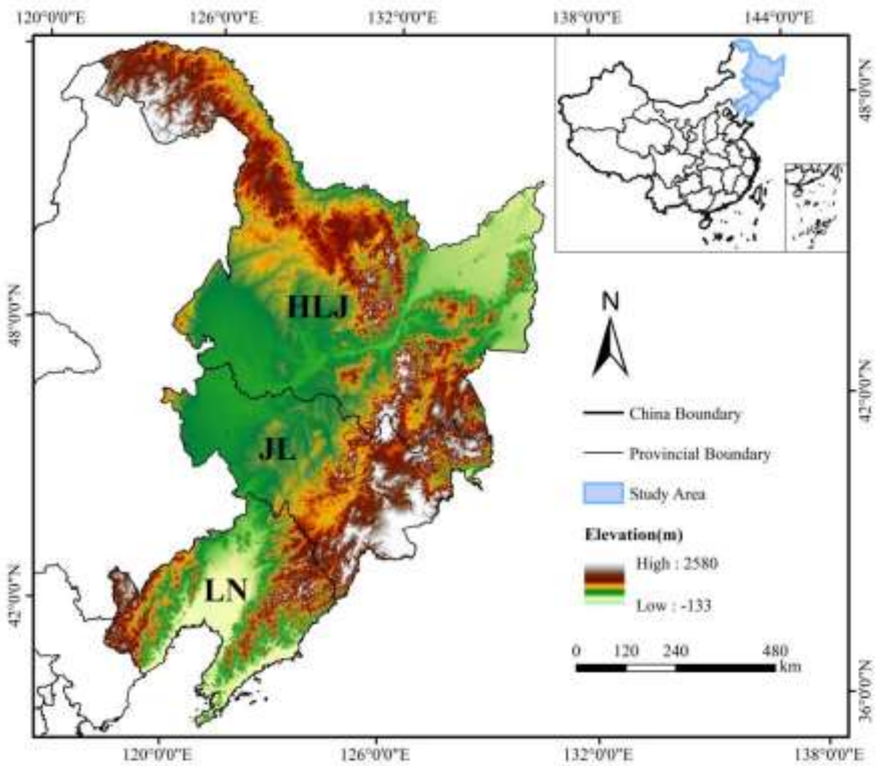

Figure 2. Map of the study area.

Landsat data and preprocessing

This study employs data from the Landsat program for large-scale crop mapping. The Landsat program is a long-term Earth observation initiative that has been in continuous operation since 1972. It consists of a series of remote sensing satellites jointly managed by the United States Geological Survey (USGS) and the National Aeronautics and Space Administration (NASA)[17]. Since the launch of Landsat-

ARTICLE IN PRESS

4, which increased the spatial resolution to 30 m, the program has provided a consistent and comparable medium-resolution remote sensing dataset spanning more than four decades. This long-term archive has become a fundamental resource for monitoring global environmental change and supporting studies on land surface processes. In this study, we use the surface reflectance products from Landsat-4/5/7/8/9. All datasets have a spatial resolution of 30 m and a revisit cycle of 16 days. Fig. 3 illustrates the effective pixel observation frequency during the growing season within the study area. The number of valid observations has increased markedly since 2000, primarily owing to advances in sensor technology and satellite availability. These continuous and increasingly dense image sequences provide a robust and reliable data foundation for crop mapping and long-term agricultural monitoring.

ARTICLE IN PRESS

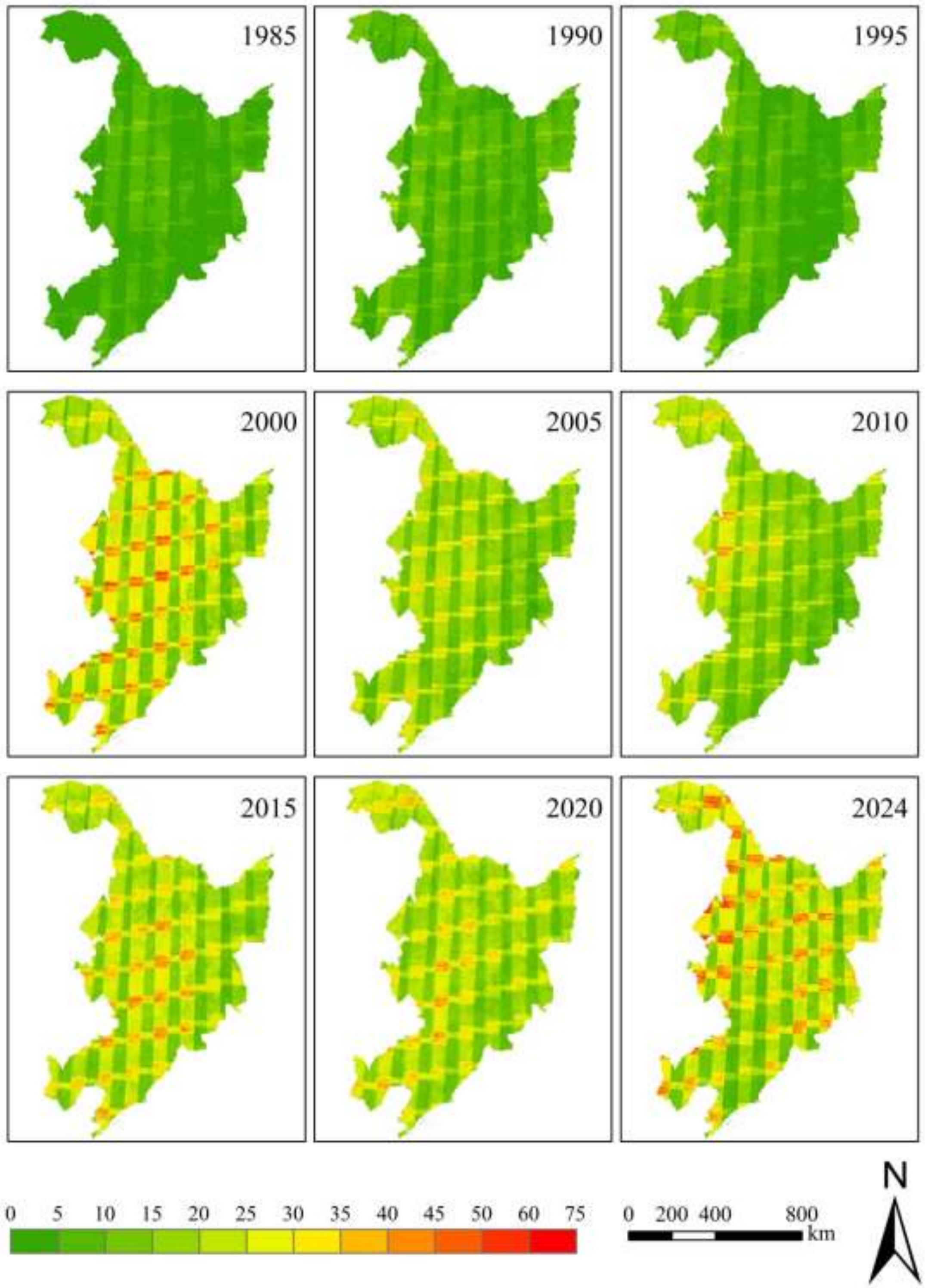

Figure 3. Observation frequency of Landsat satellites from April to October during the period 1985-2024.

All Landsat imagery used in this study underwent standardized preprocessing procedures. Cloud masking was performed following standard QA_PIXEL bit flag definitions. Low-quality pixels, primarily

ARTICLE IN PRESS

clouds and cloud shadows, were removed using the Quality Assurance (QA_PIXEL) band associated with the Landsat surface reflectance products[18]. Only clear observations were retained for subsequent analysis. Considering the phenological characteristics of the three major crops in the study region (rice, maize, and soybean), we selected Landsat observations acquired between April and October. All available Landsat observations within each month were composited using a median value composite strategy to reduce residual cloud contamination and noise. Different crop types exhibit distinct spectral signatures throughout their growth cycles. To capture these variations, we incorporated a comprehensive set of classification features, including reflectance values from the red, green, and blue bands, as well as seven agriculturally relevant spectral indices (Tab. 1). To address missing observations caused by cloud cover or data gaps, temporal interpolation was applied, followed by Whittaker smoothing to reconstruct continuous and noise-reduced time-series trajectories. These preprocessing steps ensured the consistency and reliability of long-term satellite observations for crop classification.

Table 1. Formulas for the spectral indices used in this study.

Indicator	Formula	References
NDVI	$\mathrm{NDVI} = \frac{\rho_{\mathrm{NIR}} - \rho_{\mathrm{Red}}}{\rho_{\mathrm{NIR}} + \rho_{\mathrm{Red}}}$	Tucker[19]
EVI	$\mathrm{EVI} = 2.5 \times \frac{\rho_{\mathrm{NIR}} - \rho_{\mathrm{Red}}}{\rho_{\mathrm{NIR}} + 6 \times \rho_{\mathrm{Red}} - 7.5 \times \rho_{\mathrm{Blue}} + 1}$	Huete *et al.*[20]
LSWI	$\mathrm{LSWI} = \frac{\rho_{\mathrm{NIR}} - \rho_{\mathrm{SWIR1}}}{\rho_{\mathrm{NIR}} + \rho_{\mathrm{SWIR1}}}$	Xiao *et al.*[21]
NDSVI	$\mathrm{NDSVI} = \frac{\rho_{\mathrm{SWIR1}} - \rho_{\mathrm{Red}}}{\rho_{\mathrm{SWIR1}} + \rho_{\mathrm{Red}}}$	Zheng *et al.*[22]
NDTI	$\mathrm{NDTI} = \frac{\rho_{\mathrm{SWIR1}} - \rho_{\mathrm{SWIR2}}}{\rho_{\mathrm{SWIR1}} + \rho_{\mathrm{SWIR2}}}$	Wang *et al.*[23]
GCVI	$\mathrm{GCVI} = \frac{\rho_{\mathrm{NIR}}}{\rho_{\mathrm{Red}}} - 1$	Gitelson *et al.*[24]
GWCCI	$\mathrm{GWCCI} = \mathrm{NDVI} \times \rho_{\mathrm{SWIR1}}$	Chen *et al.*[25]

*NDVI: Normalized Difference Vegetation Index; EVI: Enhanced Vegetation Index; LSWI: Land Surface Water Index; NDSVI: Normalized Difference Senescence Vegetation Index; NDTI: Normalized Difference Tillage Index; GCVI: Green Chlorophyll Vegetation Index; GWCCI: Greenness and Moisture Content Composite Index.

Training and validation data

The cropland masks generated from the high-precision cropland dataset (Tab. 2) were used to constrain the spatial extent of sample extraction. Crop samples were directly obtained from multiple crop distribution datasets, whereas samples for the "other land-cover types" category were supplemented using non-cropland areas identified in land-cover products. This approach ensured that the sample dataset accurately and rigorously represented the actual land use state across the region.

ARTICLE IN PRESS

In this study, a potential crop distribution map was first generated by integrating multiple crop classification products. This map represents a pixel-level composite that fuses multi-source crop classification information to produce a more accurate and comprehensive depiction of crop distribution than any single product alone.

Table 2. List of auxiliary datasets

Name	Spatial resolution	Data years	Data-hosting repository	References
China Land Cover Dataset (CLCD)	30m	1990-2024	https://doi.org/10.5281/zenodo.4417810	Yang *et al.*[26]
China Annual Cropland Dataset (CACD)	30m	1986-2023	https://doi.org/10.5281/zenodo.7936885	Tu *et al.*[27]
Maize, Rice, Soybean	30m	2013-2021	https://doi.org/10.6084/m9.figshare.20411424.v1	Fu *et al.*[6]
Maize, Rice, Soybean	10m	2017-2019	https://doi.org/10.6084/m9.figshare.13090442	You *et al.*[13]
Maize, Rice, Soybean	10m	2019-2023	https://code.earthengine.google.com/042b17018a2ec5983d0520bcb3104c82	Hu *et al.*[12]
Soybean	10m	2017-2021	https://doi.org/10.5281/zenod.10071427	Mei *et al.*[11]
Maize	30m	2001-2020	https://doi.org/10.57760/sciencedb.08490	Peng *et al.*[7]
Maize	30m	2016-2020	https://doi.org/10.6084/m9.figshare.17091653	Shen *et al.*[8]
Rice	30m	1990-2020	https://github.com/MKGenesis/PSPR-rice-HLJ	Zhang *et al.*[9]
Rice	20m	2017-2022	https://doi.org/10.57760/sciencedb.06963	Shen *et al.*[10]
Rice	500m	2000-2020	https://doi.org/10.5281/zenodo.5555721	Han *et al.*[28]

ARTICLE IN PRESS

This study adopts a unified approach from the outset to ensure overall consistency of data products. High-confidence pixels with complete agreement across multiple source products were selected as initial samples, establishing a set of reliable, consensus-supported sample points. For pixels exhibiting discrepancies between products, this study avoided arbitrary assignment to a single class. Instead, such pixels were labeled as “mixed” at the sampling stage and subsequently excluded, preventing erroneous data from entering the training process. Based on this harmonized sample library, a single set of features and a uniform classification algorithm were applied to the same input data, fully utilizing the continuous temporal information available in the remote sensing imagery. This approach ensures every pixel is

ARTICLE IN PRESS

classified according to identical standards, data foundations, and algorithmic procedures. This procedure establishes a robust and quality-controlled foundation for subsequent sample selection and analysis.

After completing the preliminary processing steps, cropland masking was first applied to the potential crop distribution dataset to delineate the boundaries of cropland. Random sampling was then conducted within these cropland areas. For each randomly generated candidate point, a buffer zone was constructed around the point, and the proportion of the target crop type within the buffer was calculated. A candidate point was retained as a valid crop sample only if the target crop covered at least 80% of the buffer area. Subsequently, consistency checks were performed on the initially retained samples to remove points exhibiting classification inconsistencies across data sources [9,12]. From the remaining high-confidence samples, those labeled as maize, soybean, rice and other crops were extracted and used as training samples for the four target crop categories. To ensure sufficient category diversity in the training dataset, we further incorporated non-crop samples by referencing the CLCD dataset[26]. Using this product, additional samples representing non-cropland-cover types were added, such as built-up land, grassland, forest, water bodies, and wetlands. This augmentation helps ensure that the classification results accurately represent the actual land-use conditions and enhances the robustness and reliability of subsequent crop mapping.

To construct a time-series sample database covering the entire study period, we employed an interannual sample migration approach based on the SAM method[29]. This technique extends sample points collected in a limited number of reference years to other years within the study period. The SAM algorithm is applied to the time series of the smoothed enhanced vegetation index (EVI) extracted based on Landsat images. The monthly average EVI values from April to October are selected to represent the growth dynamics of crops. To reduce noise and ensure time continuity, the Whittaker smoothing method is used to reconstruct the EVI time series. For each reference sample, the spectral similarity between its annual EVI curve and each candidate pixel in the target year is quantified using the SAM index. To enhance the robustness of the transfer process, a dual adaptive buffer strategy is adopted: first, candidate pixels are identified within a 1-kilometer radius buffer zone. If no suitable match is found, the search radius is expanded to 3 kilometers. To ensure the reliability of the transferred samples, a similarity threshold ($SAM < 0.1$) is set. Within the search area, the original category attributes of the successfully transferred samples are retained, and the SAM value and the used buffer radius are recorded. Those that do not meet the threshold are eliminated. To control the error propagation during the inter-annual data transfer process, only the pixel with the smallest SAM value within the search area is selected, and the remaining candidate pixels are eliminated. This achieves the effective reduction of the risk of classification error propagation and improves the time stability and reliability of the long-term training dataset.

To ensure the independence between training and validation samples within each year, the dataset was randomly split into training (70%) and validation (30%) subsets. The splitting was conducted at the sample level, and no overlapping samples were used in both training and validation processes for a given year. However, it should be noted that some samples were extended across multiple years through the

ARTICLE IN PRESS

interannual migration strategy, meaning that samples from the same spatial locations may appear in different years. While this may introduce a degree of temporal dependency, its impact on model evaluation is limited. This is because spectral characteristics vary substantially across years due to differences in sensors, atmospheric conditions, and crop phenology, reducing the direct transferability of learned features. Therefore, although strict spatiotemporal independence cannot be fully guaranteed, the training and validation datasets remain effectively independent for each yearly classification task.

Random Forest algorithm

Random Forest (RF) is a widely used ensemble learning algorithm that enhances the accuracy and robustness of classification and regression tasks by aggregating the predictions of multiple decision trees[30]. As the number of trees increases, the prediction error of RF converges toward the Bayes optimal error, and the algorithm exhibits particularly strong performance in additive regression models[31]. Owing to its high predictive accuracy and strong generalization capability, RF has been extensively applied in remote sensing-based crop classification[32,33].

This study employs a crop classification framework that integrates multi-temporal remote sensing imagery with probability-based decision making. First, using the monthly preprocessed images and the derived feature bands described earlier, which are designed to suppress noise and preserve stable spectral characteristics, we constructed the input feature set required for model training[34,35]. Second, independent RF classifiers were developed for each monthly composite image. Each model consisted of 100 decision trees and was trained using ground sample points. Instead of generating hard classification outputs, the models produced normalized probability distributions for each crop category at the pixel level, resulting in a series of monthly probability maps[9]. This probabilistic output preserves uncertainty information inherent in the classification process and mitigates error accumulation associated with hard-label predictions. Finally, probability fusion was performed along the temporal dimension[9]. The random forest classifier outputs the probability of each crop type on a pixel scale for each month. To obtain stable classification results within the year, the predicted probability values for each month of the growing season are averaged: the probabilities of the seven monthly graphs are averaged pixel by pixel, and then the final category of each pixel is determined based on the maximum average probability criterion, that is, the crop type with the highest average probability is selected.

Statistical analysis

This study employed a dual validation strategy to comprehensively assess the accuracy of the crop classification results. First, internal classification performance was evaluated using standard accuracy metrics derived from the confusion matrix, including overall accuracy (OA), the Kappa coefficient, producer's accuracy (PA), user's accuracy (UA), and the F1-score (F1). These metrics enable a systematic assessment of classification reliability across all crop categories. Second, an independent evaluation was conducted using official agricultural statistics. Specifically, the mapped crop areas were aggregated at provincial level and results compared with the corresponding planting area official statistics for

ARTICLE IN PRESS

ARTICLE IN PRESS

Heilongjiang, Jilin, and Liaoning provinces for the period 1998-2023. Linear regression analysis, including the Pearson correlation coefficient (R^2) and the root mean square error (RMSE), was applied to quantify the degree of consistency between the remote-sensing-derived crop area estimates and the official statistics, thereby providing an independent measure of the robustness and credibility of the mapping results.

Data Records

This study provides a series of annual crop distribution maps for the three northeastern provinces of China from 1985 to 2024 at a spatial resolution of 30 m. All datasets are publicly accessible through Zenodo[36]. The spatial coordinate system of this dataset is ESPG: 4326 (WGS_1984). The values on the maps of the three crop types are 0, 1, 2 and 3, representing respectively other land (including other crops and non-cropland), rice, maize and soybean. The spatial extent of the dataset covers the region from 38°N to 54°N and from 118°E to 136°E, encompassing the full agricultural area of the three provinces.

Technical Validation

Accuracy assessment

The validation samples were used to assess the accuracy of the crop distribution maps. Overall, the maps exhibit consistently high accuracy across provincial-level administrative regions. The classification assessment results indicate that, from 1985 to 2024, the OA for the three northeastern provinces was consistently above 0.74 (Fig. 4). In Heilongjiang Province, the OA ranged from 0.74 to 0.99. The maximum value was found in 2019 (0.99), while the lowest values occurred in 1985 and 1987 (0.74). The average OA, computed across all years, was 0.84. The Kappa coefficient varied between 0.63 and 0.97, with values below 0.70 typically found before 1990. The highest Kappa value was observed in 2017 (0.97), whereas the lowest was recorded in 1987 (0.63). The average Kappa coefficient across all years was 0.78. In Jilin Province, the OA ranged from 0.74 to 0.96, with a mean across all years of 0.81. The highest OA value occurred in 2017 (0.96). The Kappa coefficient ranged from 0.61 to 0.95 (mean of 0.73), with values below 0.70 typically found before the year 2000. The highest Kappa value was in 2017 (0.95), while the lowest was measured in 1987 (0.61). In Liaoning Province, the OA ranged from 0.79 to 0.98 (mean value 0.87). Aside from 1993, which presented the lowest value of 0.79, the accuracy exceeded 0.80 in all remaining years. A peak accuracy of 0.98 was recorded from 2017 to 2019. The Kappa coefficient ranged from 0.71 to 0.98 (mean 0.81). Several years before 2000 had values below 0.80. The highest Kappa coefficient was found in 2017, reaching 0.98, while the lowest value of 0.71 occurred in 1986.

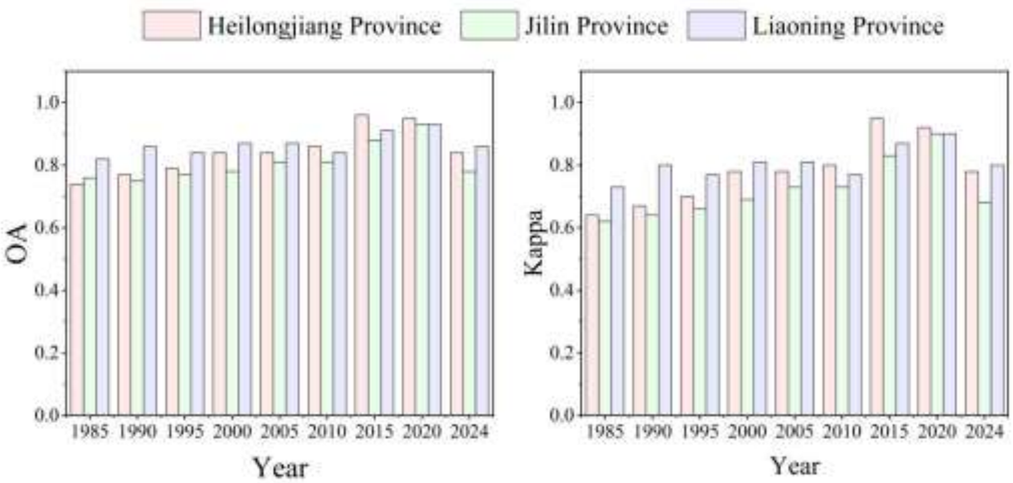

Figure 4. Overall accuracy (OA) and Kappa coefficient for Heilongjiang, Jilin, and Liaoning Provinces from 1985 to 2024.

In addition to the OA and Kappa coefficient, more comprehensive and robust evaluation metrics were introduced to further assess classification performance (Tab. 3). Specifically, Balanced Accuracy (BA) and Macro-F1 were incorporated. Compared with OA and Kappa, these metrics are less sensitive to class imbalance and can better reflect the consistency of classification performance across different categories.

Table 3 presents the BA and Macro-F1 values for Heilongjiang, Jilin, and Liaoning provinces in representative years. Overall, classification accuracy in all three provinces shows a clear increasing trend over time, although the magnitude and stability of improvement vary spatially. During the early period (1985-2000), classification accuracy was relatively low across all provinces. BA in Heilongjiang increased from 0.70 to 0.82, Jilin from 0.71 to 0.74, and Liaoning from 0.78 to 0.85, with Liaoning consistently outperforming the other two provinces. BA values were generally below 0.85 during this period, mainly due to limitations in early Landsat data quality and insufficient sample sizes.

In the middle period (2000-2010), Heilongjiang continued to improve, reaching 0.85, while Jilin and Liaoning stabilized at approximately 0.77 and 0.82, respectively. Jilin showed relatively slower improvement, primarily due to the low producer’s accuracy (PA) for soybean, which typically ranged from 0.50 to 0.65. In the recent period (after 2015), a substantial improvement was observed in all provinces. In 2015, BA reached 0.96 in Heilongjiang, 0.94 in Liaoning, and 0.88 in Jilin, with Jilin further increasing to 0.92 by 2020. Although a slight decline was observed in 2024 (Heilongjiang: 0.82, Jilin: 0.73, Liaoning: 0.86), the values remained significantly higher than those before 2000. This improvement is closely associated with the enhanced data quality of Landsat 8/9 and the increasing robustness of the sample migration method.

ARTICLE IN PRESS

ARTICLE IN PRESS

Table 3. BA of the Three Provinces and Macro F1 in Key Years.

Year	Heilongjiang		Jilin		Liaoning	
	BA	Macro-F1	BA	Macro-F1	BA	Macro-F1
1985	0.70	0.71	0.71	0.72	0.78	0.80
1990	0.73	0.74	0.71	0.72	0.84	0.85
1995	0.76	0.76	0.73	0.73	0.81	0.83
2000	0.82	0.82	0.74	0.75	0.85	0.86
2005	0.82	0.83	0.77	0.78	0.84	0.85
2010	0.85	0.85	0.77	0.79	0.82	0.83
2015	0.96	0.96	0.88	0.88	0.94	0.94
2020	0.94	0.93	0.92	0.93	0.92	0.92
2024	0.82	0.83	0.73	0.75	0.86	0.86

Assessment of crop-specific classification metrics revealed clear spatial differences among provinces, with classification performance varying across regions and crop types, as illustrated in Fig. 5. For rice, the producer accuracy (PA), user accuracy (UA), and F1-score (F1) in the three northeastern provinces consistently remained above 0.70 after the year 2000. Prior to 2000, however, the classification accuracy for rice declined noticeably. Heilongjiang Province exhibited comparatively weaker performance during this early period, whereas Liaoning Province showed markedly stronger results. In Heilongjiang Province, the minimum PA for rice reached 0.39, while UA values remained above 0.65, and the lowest F1 was 0.51. The mean PA, UA, and F1 across the full study period were 0.68, 0.86, and 0.76, respectively. In Jilin Province, PA remained above 0.60 in all years except 1991, when it reached 0.58; UA consistently exceeded 0.74, and the F1 was never lower than 0.66. The average PA, UA, and F1 values were 0.77, 0.87, and 0.82, respectively. Liaoning Province demonstrated the most stable and robust performance, with PA values consistently above 0.75, UA values no less than 0.70, and F1 always above 0.79. The corresponding mean values reached 0.85 for PA, 0.88 for UA, and 0.87 for F1.

For maize, the classification performance showed notable provincial differences. Heilongjiang Province exhibited comparatively strong accuracy, whereas Liaoning Province performed less favorably. In Heilongjiang Province, the mean producer accuracy PA, UA, and F1 reached 0.88, 0.81, and 0.84, respectively. In contrast, Liaoning Province showed lower user reliability, with corresponding mean values of 0.69 for PA, 0.86 for UA, and 0.76 for F1. Jilin Province demonstrated relatively balanced performance across metrics, with mean PA, UA, and F1 of 0.83, 0.81, and 0.82, respectively.

For soybean, Jilin Province showed comparatively weaker performance, whereas Liaoning Province achieved the highest accuracy among the three provinces. In Jilin Province, the mean producer accuracy (PA), user accuracy (UA), and F1 were 0.61, 0.80, and 0.69, respectively. In contrast, Liaoning Province

ARTICLE IN PRESS

attained substantially higher values, with mean PA, UA, and F1 of 0.92, 0.93, and 0.92. Heilongjiang Province demonstrated intermediate performance, with all three metrics averaging 0.82, indicating stable accuracy levels that fell between those of Jilin and Liaoning.

Figure 5. Producer accuracy (PA), user accuracy (UA), and F1-score for rice, maize, and soybean in Heilongjiang (HLJ), Jilin (JL), and Liaoning (LN) from 1985 to 2024.

Based on the statistical analysis of the accuracy at different stages, a further analysis from the perspective of time evolution reveals that the classification accuracy of the three provinces all showed a significant and consistent trend of improvement in stages. Among them, the improvement was most obvious from 1985-1994 to 2005-2014, and it stabilized thereafter in 2015.

In the earliest period (1985-1994), OA remains relatively low but stable across provinces (approximately 0.76-0.83), indicating a baseline level of classification capability despite limited data conditions. This stage is characterized by relatively larger discrepancies between producer accuracy (PA) and user accuracy (UA), suggesting that omission errors dominate. Such a pattern implies that the model tends to miss certain crop types rather than incorrectly labeling them, reflecting limited feature separability under sparse and noisy observations.

During the transition period (1995-2004), classification performance shows moderate improvement,

ARTICLE IN PRESS

although gains remain constrained. This stage represents a gradual enhancement in data availability and quality, but temporal observations are still insufficient to fully capture crop phenological dynamics, resulting in only incremental accuracy increases.

A substantial improvement is observed in the period 2005-2014, when overall accuracy increases markedly across all provinces. This improvement coincides with enhanced data continuity, reduced cloud contamination effects due to increased image availability, and more stable spectral representations from satellite sensors. As a result, both omission and commission errors are reduced, leading to more balanced UA and PA values.

In the most recent period (2015-2024), classification accuracy reaches a consistently high level (the OA is between 0.87 and 0.92) and stabilizes across years. The gap between UA and PA is significantly reduced, indicating a well-balanced error structure and improved reliability of crop identification.

The observed temporal pattern suggests that accuracy improvements are systematic rather than driven by isolated high-quality years, providing strong evidence for the temporal consistency of the dataset. Importantly, the lower accuracy in the pre-2000 period can be attributed to several well-understood sources of uncertainty. First, early Landsat observations are limited by low temporal frequency, frequent cloud contamination, and data gaps, which reduce the availability of valid observations during key crop growth stages and weaken phenological signal extraction. Second, differences in sensor characteristics introduce spectral inconsistencies that affect model generalization across time. Third, the sample migration strategy, which transfers training samples from data-rich recent years to earlier periods using similarity constraints, may introduce additional uncertainty due to differences in historical cropping systems and environmental conditions. Although low-confidence samples are filtered to reduce noise, this process inherently leads to conservative predictions, which is consistent with the observed dominance of omission errors (lower PA) in early periods. Furthermore, the lack of ground reference data in earlier decades limits the representativeness of training samples, further amplifying uncertainty. Despite these limitations, the gradual and consistent improvement in accuracy over time, together with the absence of abnormal fluctuations, indicates that uncertainties in early periods are systematic and bounded rather than random or biased.

To further assess the reliability of the crop distribution maps, prefecture-level statistical records from 1998 to 2023 were incorporated for independent validation of the study area (Fig. 6). The mapped crop areas for the three northeastern provinces were compared with the official statistics reported by each prefecture in each year. The results demonstrated that the dataset exhibited strong overall agreement with the statistical records. Fig. 6 presented scatter plots at five-year intervals from 2000 to 2023 to illustrate the temporal consistency of this relationship. For rice, the R^2 across the three provinces ranged from 0.80 to 0.99, and the corresponding RMSE ranged from 3.08×10^4 to 9.34×10^4 hectares. For maize, R^2 values remained above 0.82, spanning from 0.82 to 0.96, with RMSE values ranging from 7.40×10^4 to 33.04×10^4 hectares. For soybean, R^2 values exceeded 0.76, with a maximum of 0.96, and RMSE values ranged from 9.70×10^4 to 33.77×10^4 hectares. Despite the overall strong correspondence, soybean area estimates for Baicheng and Songyuan showed comparatively larger deviations. According to statistics, the area of soybean accounted for less than 1% of the total crop planting area in these two prefectures. In contrast, the cropland areas of maize, rice, oilseed crops, sunflowers, and vegetables were all larger than that of soybean. We hypothesized that some instances of peanuts, sunflowers, and vegetables may have been misclassified as soybean, which could lead to overestimation of the actual soybean planted area.

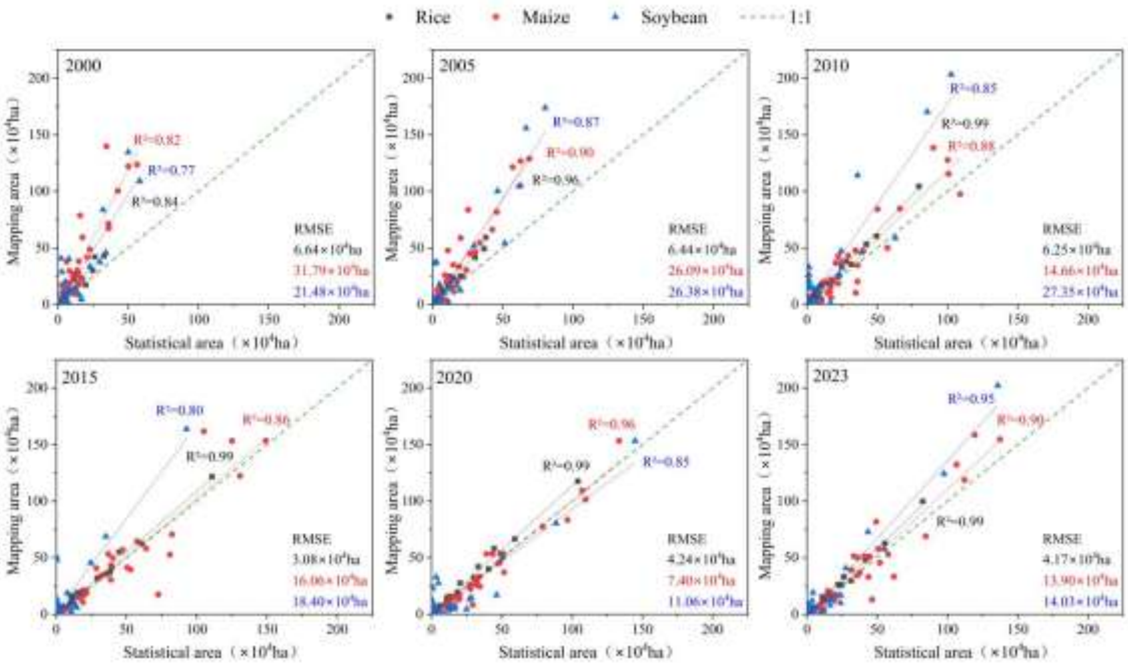

Figure 6. Comparison between mapped crop distribution and official statistical records of crop planting areas across the study region from 2000 to 2023.

Comparison with other studies

This study systematically compared the newly generated dataset with existing crop-mapping products (Tab. 2). The comparison period for maize spanned 2000-2021, for rice 2013-2022, and for soybean 2013-2021 (Fig. 7). The estimated areas of the three major grain crops (rice, maize, and soybean) in Northeast China, as derived from the crop mapping product developed in this study, demonstrate a temporal trend that is largely consistent with official statistical data. Furthermore, the results align well with the overall trends reported in existing mainstream crop products (Fig. 7). For rice and soybean in particular, our map not only captures interannual fluctuations that remain strongly synchronized with statistical data, but in multiple years produces area estimates that are closer to the statistical reference values compared to existing products. These results provide preliminary evidence supporting the

ARTICLE IN PRESS

effectiveness and potential advantages of the proposed approach in characterizing the temporal dynamics of these two crops. In contrast, the maize area estimates in our map exhibit a systematic overestimation, this situation may be attributable to several factors.

First, limitations in data continuity and model generalization played a key role. The earlier period (2001-2011) relied primarily on Landsat-5 (TM) and the malfunctioning Landsat-7 (ETM+) sensors[37], which introduced greater noise and potential calibration inconsistencies compared to the superior radiometric quality and stability of Landsat-8 (OLI) used from 2013 onward[38,39]. Furthermore, our training samples, though temporally comprehensive, may inherently better represent the crop phenotypes, management practices, and land cover contexts of the more recent years in which they were collected, leading to a gradual decline in model generalization accuracy when applied to earlier years.

Second, maize inherently presents greater fundamental mapping challenges throughout the study period, as documented in the literature[40]. The structurally complex production systems in Northeast China, particularly those involving wheat-maize rotations or maize-soybean intercropping, increase the prevalence of mixed pixels and spectral ambiguity, thereby elevating classification uncertainty[41,42]. Furthermore, the optical feature set employed here has a limited capacity to spectrally separate maize from other summer green vegetation, including certain forests and tall crops like sorghum[40]. Together, these factors contribute to the observed overestimation of maize area.

ARTICLE IN PRESS

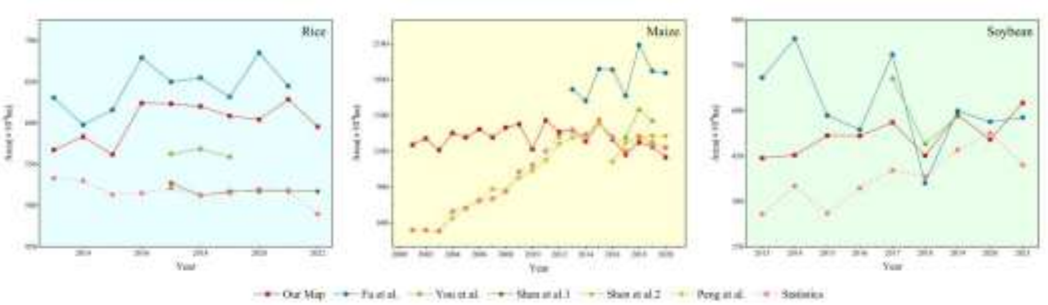

Figure 7. Comparison of the mapped areas of rice, maize, and soybean in the three northeastern provinces with existing crop products and official statistical records.

Discussion

This study primarily relies on the Landsat satellite series for crop mapping; however, the data quality exhibits clear temporal heterogeneity[9]. Due to limitations in early satellite observation conditions and the influence of cloud cover, the availability of high-quality imagery decreases progressively backward in time, a pattern that is particularly evident during the 1980s and 1990s. Previous studies have shown that, although Landsat TM data have been widely used for crop classification and mapping owing to their relatively high spatial resolution (30 m), their low revisit frequency and limited data availability constrain their application in operational crop monitoring systems. Consequently, such data are often restricted to

ARTICLE IN PRESS

local-scale classification and are less capable of supporting long-term time series analyses[43,44]. These limitations affect the feature extraction capacity of classification models, resulting in a gradual decline in classification accuracy for earlier years. This issue has been widely recognized as a common challenge in long-term remote sensing-based analyses. Furthermore, as this study integrated long-term Landsat data from multiple satellite missions (Landsat 4/5/7/8/9), it adopted surface reflectance data to enhance the consistency of radiation measurements. Although previous studies have shown that under such conditions, long-term crop mapping can still maintain stable performance through the adoption of technical strategies such as standardized preprocessing, due to the differences in spectral response functions and sensor characteristics, residual differences may still exist between different sensors[9]. These inconsistencies may introduce additional uncertainties to long-term analysis, especially in the early stages where data quality is relatively low. Future research can further enhance the comparability between different sensors by applying specialized coordination methods.

In addition, the training samples were derived from the integration of multiple crop products. To ensure sample reliability, a conservative strategy was adopted whereby only pixels with complete agreement across different datasets were retained. While this approach improves label confidence, it also leads to a more spatially concentrated sample distribution, particularly for crops such as soybean, which may introduce spatial representation bias. This, in turn, could affect the model's generalization performance in marginal areas and the robustness of the resulting maps.

Future research can apply specialized coordination methods to further enhance the comparability across sensors, integrate more satellite data sources (such as SAR data or higher-resolution optical data), to improve data continuity under cloudy conditions, enhance the representativeness of the samples through field observations, and develop regional adaptive classification frameworks. These improvements will further enhance the reliability and transferability of long-term crop mapping work.

Usage Notes

Northeast China plays a critical role in national grain production. In recent decades, continuous agricultural expansion and notable adjustments in cropping structure across the three northeastern provinces have posed potential pressures on regional water resource allocation and ecological security. Based on multi-source remote sensing data, this study constructed a long-term (1985-2024), high spatiotemporal-resolution (30 m) dataset documenting the distribution of rice, maize, and soybean.

This dataset enables long-term, spatially explicit analyses of cropping dynamics for the three major grain crops in Northeast China. Researchers can directly apply it to quantify changes in crop-specific planted area, spatial distribution patterns, and cropping system transitions (e.g., expansion, contraction, rotation) from 1985 to the present.Specific applications include: assessing the impacts of agricultural expansion and policy interventions on land use and landscape structure; serving as a critical input for

ARTICLE IN PRESS

ARTICLE IN PRESS

agro-ecosystem models to estimate crop water footprints or nutrient budgets; and providing a baseline for validating coarser-resolution land cover products. For the early (1985-2000) classification data, although affected by factors such as cloud contamination and insufficient time coverage of the Landsat satellite, the effective observations were limited, the classification accuracy was relatively low, and the uncertainty was high. However, these data still have significant value in capturing the large-scale spatial patterns and long-term change trends of crop dynamics. They are particularly suitable for regional-level analyses, such as identifying the initial distribution patterns of crops, monitoring large-scale expansion or contraction processes, and supporting trend studies at the ten-year scale under spatial or temporal aggregation. For robust application, users should note that classification confidence is higher after 2012 due to improved satellite data quality. Where precise maize acreage is required, particularly when analyzing early years in regions with complex cropping systems, supplementing the dataset with local reference data for calibration is recommended.

Code availability

JavaScript code used to generate the crop type maps are available from the Zenodo repository[36]. If you have any questions during the usage process, you can contact the author for further explanations and support.

Acknowledgements

This research was funded by the National Key Research and Development Programme of China (No. 2022YFD1500204). The opinions expressed in this work are the authors' only and cannot be taken to represent the view or positions of FAO or CAAS.

Author contributions

Zhaoyang Bai: Methodology, Code, Validation, Formal analysis, Data collection, Writing - original draft, Visualization.

Maofang Gao: Conceptualization, Writing-review & editing, Funding acquisition.

Fukang Feng: Methodology, Code, Data collection, Writing - review & editing.

Shilei Li: Writing - review & editing.

Qiang Li: Writing - review & editing.

Guofei Shang: Writing - review & editing.

Jianxi Huang: Writing - review & editing.

Zhao-Liang Li: Writing - review & editing.

Xia Zhang: Writing - review & editing.

ARTICLE IN PRESS

ARTICLE IN PRESS

Gianfausto Bottini: Writing - review & editing.

Francesco N. Tubiello: Writing - review & editing.

Competing interests

The authors declare no conflict of interest.

References

1. Cheng, Y. & Fang, Y. Morphology change and its influencing factors of agricultural terrain structure in northeast China. *Economic Geography* **30**, 1349-1353, https://doi.org/10.15957/j.cnki.jjdl.2010.08.017 (2010). [Chinese]
2. Cheng, Y. & Zhang, P. Regional patterns changes of Chinese grain production and response of commodity grain base in northeast China. *Geographical Science*, 3-10, https://doi.org/CNKI:SUN:DLKX.0.2005-05-000 (2005). [Chinese]
3. Qiu, B., Wu, F., Hu, X., Yang, P., Wu, W., Chen, J., Chen, X., He, L., Joe, B., Tubiello, F. N., Qian, J. & Wang, L. A robust framework for mapping complex cropping patterns: the first national-scale 10 m map with 10 crops in China using sentinel 1/2 images. *ISPRS Journal of Photogrammetry and Remote Sensing* **224**, 361-381, https://doi.org/10.1016/j.isprsjprs.2025.04.012 (2025).
4. Li, H., Song, X., Hansen, M. C., Becker-Reshef, I., Adusei, B., Pickering, J., Wang, L., Wang, L., Lin, Z., Zalles, V., Potapov, P., Stehman, S. V. & Justice, C. Development of a 10-m resolution maize and soybean map over China: matching satellite-based crop classification with sample-based area estimation. *Remote Sensing of Environment* **294**, 113623, https://doi.org/10.1016/j.rse.2023.113623 (2023).
5. Liu, L., Kang, S., Xiong, X., Qin, Y., Wang, J., Liu, Z. & Xiao, X. Cropping intensity map of China with 10 m spatial resolution from analyses of time-series landsat-7/8 and sentinel-2 images. *International Journal of Applied Earth Observation and Geoinformation* **124**, 103504, https://doi.org/10.1016/j.jag.2023.103504 (2023).
6. Xuan, F., Dong, Y., Li, J., Li, X., Su, W., Huang, X., Huang, J., Xie, Z., Li, Z., Liu, H., Tao, W., Wen, Y. & Zhang, Y. Mapping crop type in northeast China during 2013-2021 using automatic sampling and tile-based image classification. *International Journal of Applied Earth Observation and Geoinformation* **117** (2023).
7. Peng, Q. Y., Shen, R. Q., Li, X. Q., Ye, T., Dong, J., Fu, Y. Y. & Yuan, W. P. A twenty-year dataset of high-resolution maize distribution in China. *Scientific Data* **10** (2023).
8. Shen, R. Q., Dong, J., Yuan, W. P., Han, W., Ye, T. & Zhao, W. Z. A 30 m resolution distribution map of maize for China based on Landsat and sentinel images. *Journal of Remote Sensing* **2022** (2022).
9. Zhang, C. K., Zhang, H. Y. & Tian, S. J. Phenology-assisted supervised paddy rice mapping with the Landsat imagery on google earth engine: experiments in Heilongjiang province of China from 1990 to 2020. *Computers and Electronics in Agriculture* **212**, https://doi.org/10.1016/j.compag.2023.108105 (2023).
10. Shen, R. Q., Pan, B. H., Peng, Q. Y., Dong, J., Chen, X. B., Zhang, X., Ye, T., Huang, J. X. & Yuan, W. P. High-resolution distribution maps of single-season rice in China from 2017 to 2022. *Earth System Science Data* **15**, 3203-3222 (2023).
11. Mei, Q. H., Zhang, Z., Han, J. C., Song, J., Dong, J. W., Wu, H. Q., Xu, J. L. & Tao, F. L. ChinaSoyArea10m: a dataset of soybean-planting areas with a spatial resolution of 10 m across china from 2017 to 2021. *Earth System Science Data* **16**, 3213-3231 (2024).
12. Hu, X. Q., Zhang, S., Li, L., Huang, J. X., Zhao, Z. Y., Liu, K. Y., Zhang, Z. J. & Yao, X. C. Major grain crop mapping in northeast China using sample generation method and ensemble learning. *European Journal of Agronomy* **169** (2025).
13. You, N., Dong, J., Huang, J., Du, G., Zhang, G., He, Y., Yang, T., Di, Y. & Xiao, X. The 10-m crop type maps in northeast China during 2017-2019. *Scientific Data* **8** (2021).

ARTICLE IN PRESS

14. Lu, J., Li, J., Fu, H. K., Tang, X. H., Liu, Z., Chen, H., Sun, Y. & Ning, X. Y. Deep learning for multi-source data-driven crop yield prediction in Northeast China. *Agriculture-Basel* **14** (2024).
15. Zhai, Y. G., Wang, N., Zhang, L. F., Hao, L. & Hao, C. H. Automatic crop classification in Northeastern China by improved nonlinear dimensionality reduction for satellite image time series. *Remote Sensing* **12** (2020).
16. Liu, B. Y., Zhang, G. L., Xie, Y., Shen, B., Gu, Z. J. & Ding, Y. Y. Delineating the black soil region and typical black soil region of Northeastern China. *Chinese Science Bulletin* **66**, 96-106 (2021).
17. Wang, S., Azzari, G. & Lobell, D. B. Crop type mapping without field-level labels: random forest transfer and unsupervised clustering techniques. *Remote Sensing of Environment* **222**, 303-317 (2019).
18. Hao, P. Y., Tang, H. J., Chen, Z. X., Meng, Q. Y. & Kang, Y. P. Early-season crop type mapping using 30-m reference time series. *Journal of Integrative Agriculture* **19**, 1897-1911 (2020).
19. Tucker, C. J. Red and photographic infrared linear combinations for monitoring vegetation. *Remote Sensing of Environment* **8**, 127-150 (1979).
20. Huete, A., Didan, K., Miura, T., Rodriguez, E. P., Gao, X. & Ferreira, L. G. Overview of the radiometric and biophysical performance of the MODIS vegetation indices. *Remote Sensing of Environment* **83**, 195-213 (2002).
21. Xiao, X. M., Boles, S., Liu, J. Y., Zhuang, D. F., Frolking, S., Li, C. S., Salas, W. & Moore, B. I. Mapping paddy rice agriculture in southern China using multi-temporal MODIS images. *Remote Sensing of Environment* **95**, 480-492 (2005).
22. Zheng, B., Campbell, J. B. & de Beurs, K. M. Remote sensing of crop residue cover using multi-temporal Landsat imagery. *Remote Sensing of Environment* **117**, 177-183 (2012).
23. Wang, L. L., Hunt, E. R., Qu, J. J., Hao, X. J. & Daughtry, C. Remote sensing of fuel moisture content from ratios of narrow-band vegetation water and dry-matter indices. *Remote Sensing of Environment* **129**, 103-110 (2013).
24. Gitelson, A. A., Gritz, Y. & Merzlyak, M. N. Relationships between leaf chlorophyll content and spectral reflectance and algorithms for non-destructive chlorophyll assessment in higher plant leaves. *Journal of Plant Physiology* **160**, 271-282 (2003).
25. Chen, H., Li, H. P., Liu, Z., Zhang, C., Zhang, S. Q. & Atkinson, P. M. A novel greenness and water content composite index (GWCCI) for soybean mapping from single remotely sensed multispectral images. *Remote Sensing of Environment* **295** (2023).
26. Yang, J. & Huang, X. The 30 m annual land cover dataset and its dynamics in China from 1990 to 2019. *Earth System Science Data* **13**, 3907-3925 (2021).
27. Tu, Y., Wu, S. B., Chen, B., Weng, Q. H., Bai, Y. Q., Yang, J., Yu, L. & Xu, B. A 30 m annual cropland dataset of China from 1986 to 2021. *Earth System Science Data* **16**, 2297-2316 (2024).
28. Han, J. C., Zhang, Z., Luo, Y. C., Cao, J., Zhang, L. L., Zhuang, H. M., Cheng, F., Zhang, J. & Tao, F. L. Annual paddy rice planting area and cropping intensity datasets and their dynamics in the Asian monsoon region from 2000 to 2020. *Agricultural Systems* **200** (2022).
29. Li, X., Yu, L., Peng, D. & Gong, P. A large-scale, long time-series (1984-2020) of soybean mapping with phenological features: Heilongjiang province as a test case. *International Journal of Remote Sensing* **42**, 7332-7356 (2021).
30. Biau, G. & Scornet, E. A random forest guided tour. *Test* **25**, 197-227 (2016).
31. Scornet, E., Biau, G. & Vert, J. P. Consistency of random forests. *Ann. Stat.* **43**, 1716-1741 (2015).
32. Raja, S. P., Sawicka, B., Stamenkovic, Z. & Mariammal, G. Crop prediction based on characteristics of the agricultural environment using various feature selection techniques and classifiers. *IEEE Access* **10**, 23625-23641 (2022).
33. Shi, L., Qin, Y. Q., Zhang, J. J., Wang, Y., Qiao, H. B. & Si, H. P. Multi-class classification of agricultural data based on random forest and feature selection. *Journal of Information Technology Research* **15**, https://doi.org/10.4018/JITR.298618 (2022).
34. Xin, Q., Zhang, L. Q., Qu, Y., Geng, H., Li, X. G. & Peng, S. W. Satellite mapping of maize cropland in one-season

ARTICLE IN PRESS

ARTICLE IN PRESS

planting areas of China. *Scientific Data* **10** (2023).

35. Hao, P. Y., Löw, F. & Biradar, C. Annual cropland mapping using reference Landsat time series-a case study in central Asia. *Remote Sensing* **10** (2018).
36. Bai, Z. Y., Gao, M. F., Feng, F. K., Li, S. L., Li, Q., Shang, G. F., Bottini, G. & Tubiello, F. N. Long-term crop mapping in the three provinces of Northeast China based on multi-source sample fusion. *Zenodo*, https://doi.org/10.5281/zenodo.17595755 (2025).
37. Lee, S., Cho, M. & Lee, C. An effective gap filtering method for Landsat ETM plus SLC-off data. *Terrestrial, Atmospheric and Oceanic Sciences* **27**, 921-932 (2016).
38. Dong, J., Xiao, X., Kou, W., Qin, Y., Zhang, G., Li, L., Jin, C., Zhou, Y., Wang, J., Biradar, C., Liu, J. & Moore, B. Tracking the dynamics of paddy rice planting area in 1986–2010 through time series Landsat images and phenology-based algorithms. *Remote Sensing of Environment* **160**, 99-113, https://doi.org/10.1016/j.rse.2015.01.004 (2015).
39. Rozenstein, O. & Karnieli, A. Comparison of methods for land-use classification incorporating remote sensing and GIS inputs. *Applied Geography* **31**, 533-544, https://doi.org/10.1016/j.apgeog.2010.11.006 (2011).
40. Li, X. Y., Yu, L., Du, Z. R. & Liu, X. X. Crop statistic to annual map: tracking spatiotemporal dynamics of crop-specific areas through machine learning and statistics disaggregating. *Scientific Data* **12** (2025).
41. Zhang, D., Wu, T., Li, M., Guo, Y., Luo, J. & Dong, W. Remote sensing-based classification of crops on a farmland parcel scale and uncertainty analysis. *Remote Sensing for Natural Resources* **36**, 124-134, https://doi.org/10.6046.zrzyyg.2023166 (2024). [Chinese]
42. Song, Q., Hu, Q., Zhou, Q. B., Hovis, C., Xiang, M. T., Tang, H. J. & Wu, W. B. In-season crop mapping with GF-1/WFV data by combining object-based image analysis and random forest. *Remote Sensing* **9** (2017).
43. De la Casa, A. C. & Ovando, G. G. Estimation of wheat area in Córdoba, Argentina, with multitemporal NDVI data of SPOT-vegetation. *International Journal of Geosciences* **4**, 1355-1364 (2013).
44. De Wit, A. & Clevers, J. Efficiency and accuracy of per-field classification for operational crop mapping. *Int. J. Remote Sensing* **25**, 4091-4112 (2004).

ARTICLE IN PRESS